Materials Research Bulletin 45 (2010) 1263–1270

Contents lists available at ScienceDirect

Materials Research Bulletin

journal homepage: www.elsevier.com/locate/matresbu

A novel nanostructured composite formed by interaction of copper octa(3-aminopropyl)octasilsesquioxane with azide ligands: Preparation, characterization and a voltammetric application

Devaney Ribeiro do Carmo [a,*], Leonardo Lataro Paim [b], Gustavo Metzker [c], Newton Luiz Dias Filho [a], Nelson Ramos Stradiotto [b]

[a] Faculdade de Engenharia de Ilha Solteira UNESP – Univ Estadual Paulista, Departamento de Física e Química, Av. Brasil Centro, 56 CEP 15385-000, Ilha Solteira, SP, Brazil
[b] Instituto de Química de Araraquara UNESP – Univ Estadual Paulista, Rua Francisco Degni s/n, CEP 14801-970, Araraquara, SP, Brazil
[c] Instituto de Química de São Carlos, Universidade de São Paulo, Av. Trabalhador Sao-carlense, 400, 13566-590 São Carlos, SP, Brazil

ARTICLE INFO

Article history:
Received 17 June 2009
Received in revised form 2 May 2010
Accepted 6 May 2010
Available online 15 May 2010

Keywords:
A. Nanostructures
A. Composites
B. Chemical synthesis
B. Electrochemical properties
C. Electrochemical measurements

ABSTRACT

This study presents the preparation, characterization and application of copper octa(3-aminopropyl)octasilsesquioxane following its subsequent reaction with azide ions (ASCA). The precursor (AC) and the novel compound (ASCA) were characterized by Fourier transform infrared spectra (FTIR), nuclear magnetic resonance (NMR), electron paramagnetic resonance (EPR), scanning electronic microscopy (SEM), X-ray diffraction (XRD), Thermogravimetric analyses and voltammetric technique. The cyclic voltammogram of the modified graphite paste electrode with ASCA (GPE–ASCA), showed one redox couple with formal potential ($E_{1/2}^{\mathrm{ox}}$) = 0.30 V and an irreversible process at 1.1 V (*vs.* Ag/AgCl; NaCl 1.0 M; $\nu = 20\,\mathrm{mV\,s^{-1}}$). The material is very sensitive to nitrite concentrations. The modified graphite paste electrode (GPE–ASCA) gives a linear range from 1.0×10^{-4} to 4.0×10^{-3} mol L^{-1} for the determination of nitrite, with a detection limit of 2.1×10^{-4} mol L^{-1} and the amperometric sensitivity of 8.04 mA/mol L^{-1}.

1. Introduction

Octahedral or cubic silsesquioxanes (cubes) and the related polyhedral oligomeric silsesquioxanes (POSS) are nano-sized inorganic materials with a silica core and reactive functional groups on the surface. The silsesquioxane [1,2] has an empirical formula $(RSiO_{1.5})_n$, where R may be a hydrogen or some organic group such as alkyl, methyl, aryl, vinyl, phenyl or any organofunctional derivative from these organic groups. Each silicon atom is, on average, connected to three oxygen atoms and to an R group (hydrocarbon). When $n = 4$, 6, 8, 10 ($n \geq 4$), the resulting compounds are called polyhedral oligomeric silsesquioxanes [1–7] (POSS).

In contrast to siloxane, silsesquioxanes (SQS) can occur as cubic, ladder- or cage-type nanostructures [6,7]. The strong intermolecular forces between their constituent molecules and neighbors, as well as their strong framework with shorter bond lengths, make these silica nanocomposites even more resistant to chemical degradation.

Polyhedral oligosilsesquioxanes (POSS) have currently incited considerable interest because of their wide ranging application potentials, such as in inorganic/organic hybrid materials precursors (ormosils or ormocers) [2,3].

Cubic silsesquioxane $R_8Si_8O_{12}$, consists of a rigid, crystalline silica-like core that is perfectly defined spatially (0.5–0.7 nm) and that can be linked covalently to eight R groups which can be replaced by similar or different functional groups to form multifunctional materials with intermediate properties between those of organic polymers and of ceramics.

The most common applications are those that have technological significance, such as additives [8–12] (crossed bonds agents and thermal and viscosity modifiers); precursory for polymer dendrimers and transition metal complex octafunctional silsesquioxanes [13–18] (medical materials, advanced plastics and elastomeric resins); liquid crystals [19,20]; electroactive films [21]; biosensors [22] precursory for silicon interface [6]; glass and ceramic matrixes [23]; homogenous and heterogeneous catalysts [24,25] and more recently material for biomedical applications [26].

In the octa(3-aminopropyl)octasilsesquioxane (2) (Fig. 1) the cubic silica core is rigid and completely defined, and the eight ammine organic functional groups are appended to the vertexes

---

[*] Corresponding author. Tel.: +55 1837431076; fax: +55 18 3742 4868.
E-mail address: docarmo@dfq.feis.unesp.br (D.R. do Carmo).

0025-5408/$ – see front matter © 2010 Elsevier Ltd. All rights reserved.
doi:10.1016/j.materresbull.2010.05.005

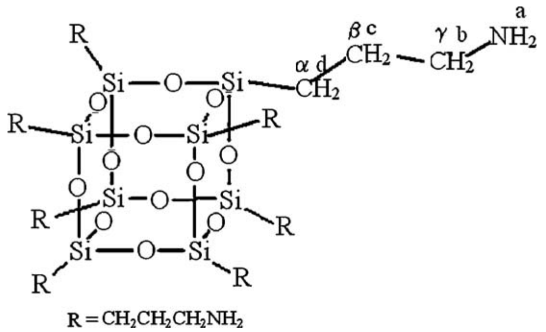

Fig. 1. Structure of octa(3-aminopropyl)octasilsesquioxane. The top symbol denote ^{13}C (α, β, γ) and ^{1}H (a, b, c, d) NMR signal.

of the cube via spacer linkages. All eight functional groups of (2) are unable to attach to the same nanoparticle due to the steric hindrance of the cubic structure. Thus, (2) should act as a cubic linker for the nanoparticles. The material synthesized in this manner serves as precursor for a series of other composites via chemical reaction with different types of synthesis. In addition, the silsesquioxane structure ($Si_8O_{12}^-$) is an electron acceptor that has been compared to the group CF_3^- [27]. Thus, the first objective of this research work was the preparation and characterization of copper octa(3-aminopropyl)octasilsesquioxane following its subsequent reaction with azide ions. Metal particles in the nanometer range exhibit quantum mechanical properties, rendering them promising candidates for nanotechnology applications [28]. Recently, the chemistry of azide complexes has become a field of rising interest. The preparation and identification of the numerous azide compounds have currently been reported [29–33]. Azide ions are interesting versatile ligands, their bonding in transition metal centers has generated various magnetic materials. After the preparation and characterization of azido copper octa(3-aminopropyl)octasilsesquioxane, the novel material was tested as a sensor for nitrite, using the cyclic voltammetry technique, therefore this study proposes a simple method for the preparation of nanohybrid materials with an electroanalytical sensor as a potential candidate.

2. Materials and methods

2.1. Reagents

All chemicals were of analytical reagent grade. All solutions and supporting electrolytes were prepared using doubly-demineralized water obtained by passing distilled water through a Millipore Milli-Q water purification system. The other reagents and solvents were of analytical grade (Sigma–Aldrich, Merck) and were used as purchased.

2.2. Synthesis

2.2.1. Preparation of octa(3-aminopropyl)octasilsesquioxane (AC)

Octa(3-aminopropyl)octasilsesquioxane (AC) was prepared according to the procedure described in the literature [34] with some modifications.

The preparation of octa(3-aminopropyl)octasilsesquioxane used a two-step process.

- *Step 1*. Concentrated HCl (200 mL) was carefully added, under stirring, to a solution. A 150 mL syringe containing γ-aminopropyltriethoxysilane ($H_2NCH_2CH_2CH_2Si(OEt)_3$) was slowly added to methanol anhydrous (3.6 L) in a 4.0 L three-neck round bottom flask. The bottle was capped and allowed to stand for 6 weeks at 30 °C. The product usually begins to crystallize from the reaction mixture after 3–4 weeks. A solution of octahydrochloride salt in 31%, was obtained and washed with cold methanol and then dried at room temperature. The resulting product, the octahydrochloride salt, was designated (1).
- *Step 2*. A neutralization of (1). Amberlite IRA-400 (Cl) ion-exchange resin (37 g) was prepared by successive washing with water (4 × 200 mL), 1 M NaOH (3 × 200 mL), water (6 × 200 mL). The resin was suspended in an eluent and chilled (−10 °C; 2 h) before use. Half of the resin beads were loaded onto a column (3.5 cm outside diameter); the other half was used to dissolve a suspension of (1). The elution across the column produced a stock solution that was tested negative for chloride. To avoid decomposition the amine should be prepared immediately before use and stored in methanol solutions at −35 °C. The purity and identity of these compounds was confirmed by conventional analytical methods (microanalysis (C, N, H), infrared (FTIR) and absorption spectroscopy).

2.2.2. Preparation of azido copper octa(3-aminopropyl) octasilsesquioxane

The compound copper octa(3-aminopropyl)octasilsesquioxane was prepared by the following procedure: 163 mg of $CuCl_2 5\cdot H_2O$ was added to a methanolic solution of $[H_2N(CH_2)_3]_8Si_8O_{12}$ (10 mL), and the blue transparent solution was stirred for 2.5 h at room temperature, next, a solution of 74 μL of saturated sodium azide was added to form a green precipitate. (Caution! Azide complexes are potentially explosive. Only a small amount of the material should be prepared and always handled with care.) In order to prevent a possible thermal degradation, this gelatinous green precipitate was filtered through a celite bed, washed with methanol and water five times, respectively and finally lyophilized (the azide compound is thermally unstable). The dried product was stored and sheltered from light. The resulting composite was designated as ASCA.

3. Techniques

3.1. NMR solid state analyses

All ^{29}Si (59.5 MHz) and ^{13}C NMR (75.4 MHz) solid state analyses were recorded on a Varian INOVA 300 spectrometer. The samples were packed in zirconia rotors and spun at the magic angle at 4500 Hz, after a relaxation delay of 10.0 and 6.0 s for ^{29}Si and ^{13}C respectively. ^{1}H were recorded in $CDCl_3$ medium. All chemical shifts in the spectra were reported in units (ppm) using tetramethylsilane (TMS) as an external reference.

3.2. Fourier transform infrared spectra (FTIR)

Fourier transform infrared spectra (FTIR) were recorded on a Nicolet 5DXB FTIR 300 spectrometer. Approximately 600 mg of KBr was ground using a mortar and pestle, and a sufficient amount of solid sample was ground with KBr to make a 1 wt% mixture to produce KBr pellets. After the sample was loaded, the sample chamber was purged with nitrogen for a minimum of 10 min before data collecting. A minimum of 64 scans was collected for each sample at a resolution of $\pm 4\ cm^{-1}$.

3.3. X-ray diffraction (XRD)

The X-ray diffraction patterns (XRD) were obtained using a Siemens D 5000 diffractometer with Cu Kα radiation, submitted to 40 kV, 30 mA, $0.05^\circ\ s^{-1}$ and exposed to radiation from 10° to 40° (2θ).

3.4. Electron paramagnetic resonance analyses

Electron paramagnetic resonance analyses (EPR) were recorded on a Bruker ESP 300E spectrometer X-band at 77 K.

3.5. Scanning electron microscopy

The scanning electron microscopy (SEM) of the materials was obtained using a JEOL JSM T-300 microscope. The samples were adhered over aluminum holders and covered with a thin layer (20–30 nm) of gold in Sputter Coater Bal-Tec SCD-050.

3.6. Thermal analyses

Thermogravimetry (TG) was performed with a Mettler 181 thermoanalyser. The samples (5–10 mg) were placed in platinum sample holders. The runs were performed under nitrogen stream (50 mL/min) and still air. Then the samples were heated at a ramp of 10 °C/min to the final temperature of 1200 °C.

3.7. Electrochemical measurements

Cyclic voltammograms were performed using the Microquimica (MQP1-PGST) potentiostat. The three electrode systems used in these studies consisted of a modified working electrode (graphite paste electrode), an Ag/AgCl reference electrode, and a platinum wire as the auxiliary electrode. The measurements were carried out at 25 °C. The graphite paste electrode modified with ASCA (GPE–ASCA) was prepared by mixing 10 mg of ASCA with 90 mg of graphite (Aldrich) and 50 μL of mineral oil. The electrode body was produced from a glass tube of 3 mm i.d. and 14 cm height, containing graphite paste. A copper wire was inserted through the opposite end of the glass tube to establish electrical contact.

After homogenizing the mixture, the modified paste was carefully positioned on the tube tip to avoid possible air gaps, which often enhances electrode resistance. The external surface of the electrode was smoothed on soft paper. A new surface can be produced by scraping out the old surface and replacing the carbon paste.

3.8. Electroanalytical procedure

Initially, cyclic voltamograms were recorded to study the sensibility of nitrite by graphite paste electrode modified with ASCA. The nitrite solutions were prepared immediately before use and were deaerated with nitrogen. In most of the experiments, 1.0 mol L^{-1} NaCl (pH ~ 6.9) was used as the supporting electrolyte. The catalytic current was estimated by the difference in the electrode current in the presence of analite compound and that established the blank solution.

4. Results and discussion

Compound (2) was synthesized by the hydrolytic condensation reaction of aminopropyltriethoxysilane in acid aqueous methanol. The characterization of ASCA was first studied using FTIR spectroscopy. Fig. 2 illustrates the vibrational spectrum of (A) AC; (B) sodium azide and (C) ASCA. The vibrational spectrum of ASCA (C) presents some absorptions corresponding to the octa(3-aminopropyl)octasilsesquioxane (A) and a new strong absorption at 2033 cm^{-1} is attributed to the asymmetric stretching ($\nu_{asym}(N_3)$) shifted about 98 cm^{-1} with relation to the isolated azide ($\nu_{asym}(N_3)$) [35]. The difference between the (B) and (C) spectra is in the region between 1300 and 1000 cm^{-1}. In this

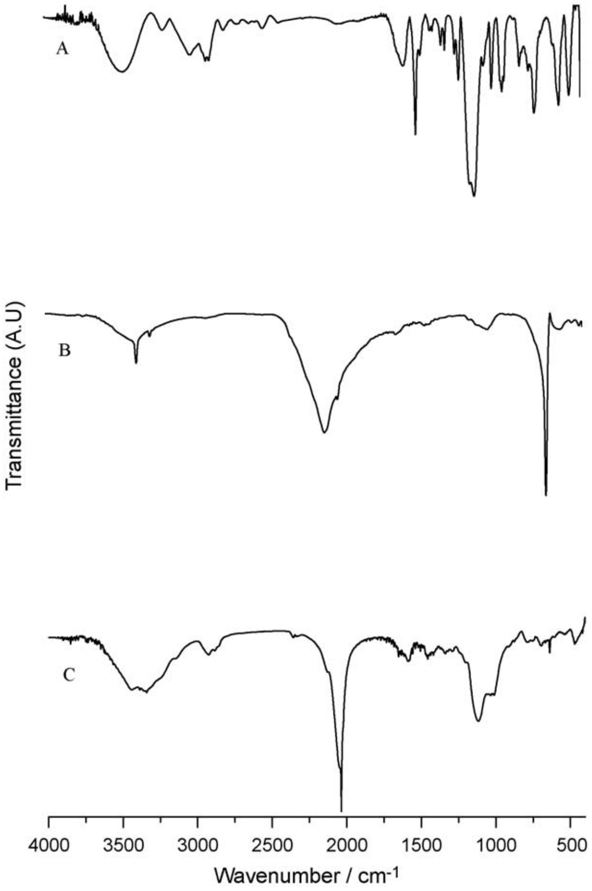

Fig. 2. Infrared for composites: sodium azide (A) and ASCA (B).

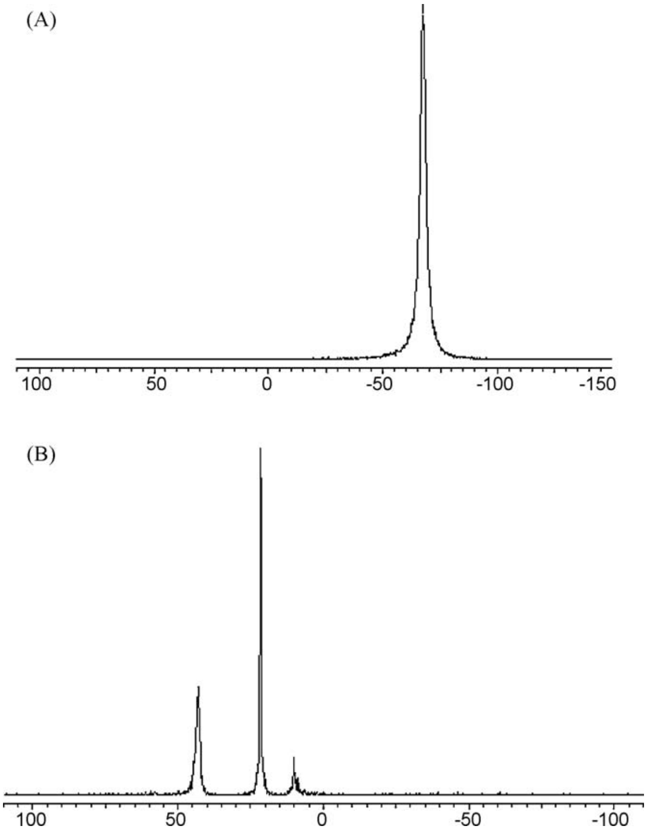

Fig. 3. ^{29}Si and ^{13}C nuclear magnetic resonance solid state for AC.

Table 1
Main spectroscopic data for $[NH_2(CH_2)_3SiO_{1.5}]_8$.

FTIR (cm^{-1})	^{13}C NMR (ppm)	^{13}Si NMR (ppm)	^{1}H NMR (ppm)
Si–O–Si: 1110–1130 N–H: 1650–3500 C–N: 1490 C–Si: 1253 C–Si: 765 C–H: 2950 C–H: 1387–1408	α-C: 10.18 β-C: 21.67 γ-C: 43.19	SiO_2: −66.5	a-N$\underline{H}_2$: 7.8 b-C$\underline{H}_2$: 2.9 c-C$\underline{H}_2$: 1.8 d-C$\underline{H}_2$: 0.72

region, the bending-groups in the azide bands were not clearly identifiable in the spectrum of the hybrid material (C), because they overlap with the broad bands of Si–O–Si (A).

The only sharp symmetrical peak (−66.5 ppm) in ^{29}Si NMR and three characteristic peaks in ^{13}C NMR spectra indicate that (1), which has a cage-like structure, was successfully synthesized. The three CH_2 groups (α, β, γ) to the terminal silicon atom, were clearly seen in the ^{13}C NMR (α-CH_2 at 10.18, β-CH_2 at 21.67 and γ-CH_2 at 43.19 ppm) (Fig. 3). ^{1}H NMR spectrum supports the characterization (a-NH_2 at 7.8, b-CH_2 at 2.9, c-CH_2 at 1.8 and d-CH_2 at 0.72 ppm). Elemental analysis (%): theoretical value C: 32.73; H: 7.27; N: 12.73. Measurement value C: 32.75; H: 7.32; N: 12.71. Table 1 lists a summary of the spectroscopic data for $[NH_2(CH_2)_3SiO_{1.5}]_8$.

The reaction of (2) with azide ions was performed using a Lewis acid–base interaction. To form the modified silsesquioxane described here as ASCA the peripheral arms with copper interact with the weak base (N_3^-). The atomic absorption spectroscopy (AAS) of the ASCA was consistent with a 1:2 silsesquioxane to copper ratio. The elemental analysis (%) for ASCA was: measurement value: C: 26.29; H: 5.29; N: 18.17, these values are in good agreement for established 1:2 silsesquioxane to copper ratio.

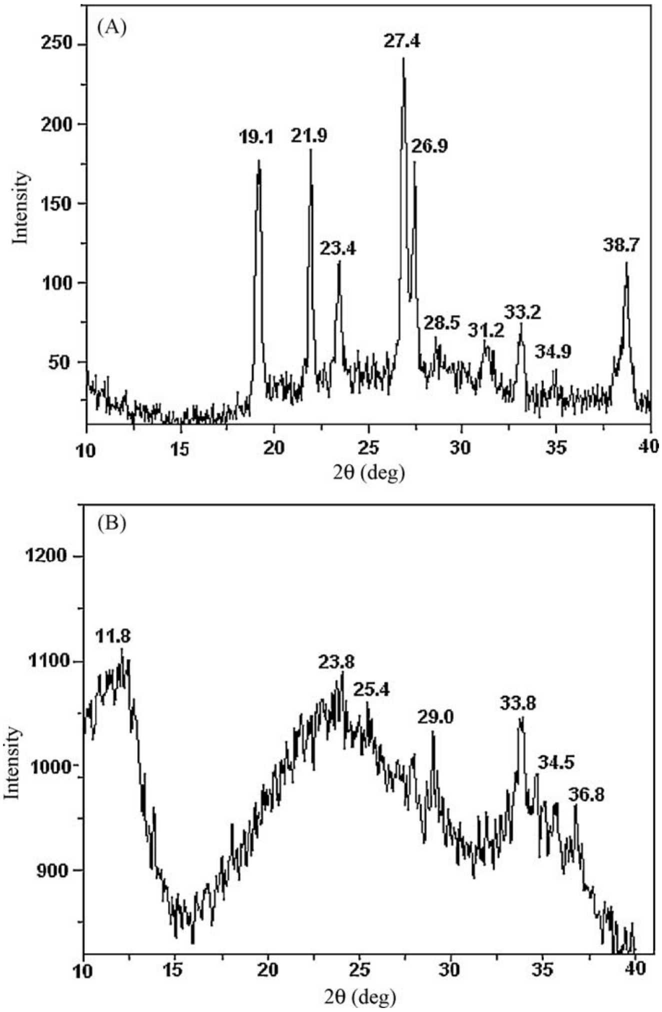

Fig. 4. XRD for AC (A) and ASCA (B).

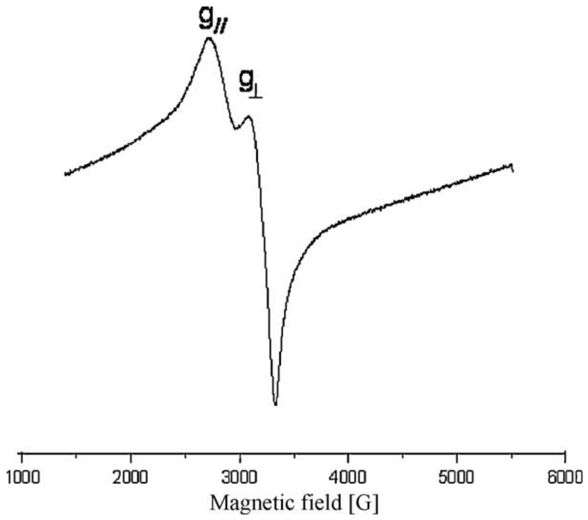

Fig. 5. EPR spectra of ASCA at room temperature.

The structural effect of ASCA was also verified through X-ray diffraction (XRD). Fig. 4 illustrates the diffractograms obtained before (A) and after (C) the modification of silsesquioxane. The X-ray diffraction spectra (XRD) for AC and ASCA are illustrated in Fig. 4(A) and (B), with the following characteristics 2θ (°) at 19.1; 21.9; 23.4; 27.4; 26.9; 28.5; 31.2; 34.9; 38.7; and 11.8; 23.8; 25.4; 29.0; 33.8; 36.8, respectively. Broadened features are clearly observed,

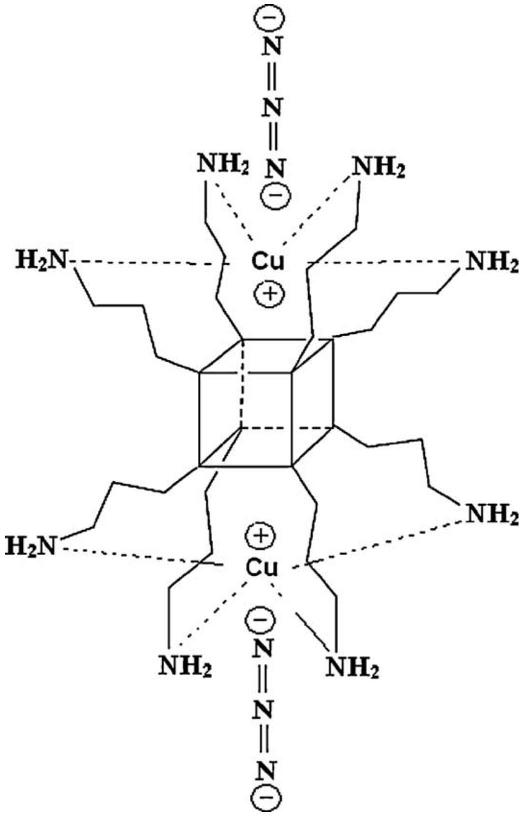

Fig. 6. Schematic representation of ASCA.

indicating that the products are not in the totally amorphous state and some repeated units are involved, although crystallinity is not high. In agreement with Lichtenhan and co-workers [36] a redistribution of the silicon environment is accompanied by remarkable increases in the line widths as well as shifts in their maximum values.

Cu^{2+} was found to react stronger with N_3^- among several transition metals commonly contained in biological fluids. In addition, ion Cu^{2+} offers some advantageous features for the application of EPR spectroscopy. The $3d^9$ configuration ($S = 1/2$) in its ionized state (Cu^{2+}) makes its EPR signal sensitive to ligand substitution. Thus, making it possible to obtain information about the structure and the nature of the interaction between N_3^-/copper silsesquioxane complex [37].

EPR of ASCA, illustrated in Fig. 5, at room temperature, indicates that this material contains mostly uncoupled monomeric species between its copper centers, different that at lower concentrations, therefore, the EPR spectrum is mainly due to uncoupled monomeric species [38].

In the present study, as exhibited in Fig. 5, there is an absence of the characteristic hyperfine structure of Cu^{2+} system. The absence of hyperfine structure is explained by the high concentration of copper and the change of interactions among copper, azide and nitrogen atoms found in the nanocomposite, which can increase other interaction types besides the hyperfine interactions. The tensor components $g_\perp$ and $g_{//}$ values for ASCA were 2.13 and 2.30, respectively. The $g_{//}$ can be assigned to Cu^{2+} ions in the distorted octahedral coordination sphere containing nitrogen atoms [39].

A possible schematic representation of the composite ASCA is illustrated in Fig. 6. This suggested representation is in agreement with the results of AAS, microanalyses, ^{13}C and ^{29}Si NMR MAS, FTIR, RPE spectroscopies.

The SEM of the ASCA shows a clear distribution of the particles into two different phases. The top and bottom surface of the crystals have an equal length (3 μm) (see Fig. 7) and this was attributed to a conductor phase due to the copper ions. The internal phase has homogeneous microparticles.

Thermogravimetric analysis of the AC and ASCA under nitrogen displayed three weight losses (Fig. 8). Tables 2 and 3 list the main thermogravimetrical data for both composites.

Under inert atmosphere the AC and ASCA decomposition starts at about 115 and 107 °C, respectively and over 650 °C a levelling of weight loss is observed for both.

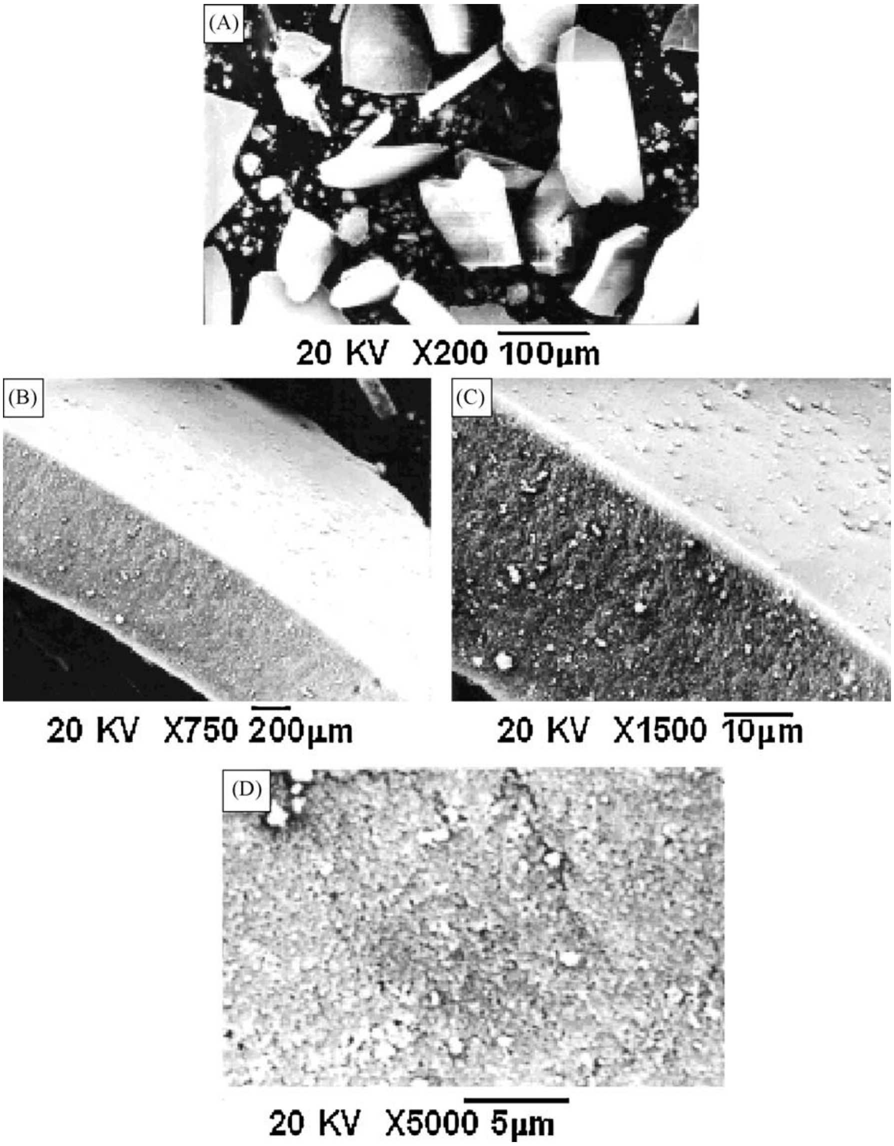

Fig. 7. Scanning electron micrograph of ASCA: A (200×); B (750×); C (1500×); D (5000×).

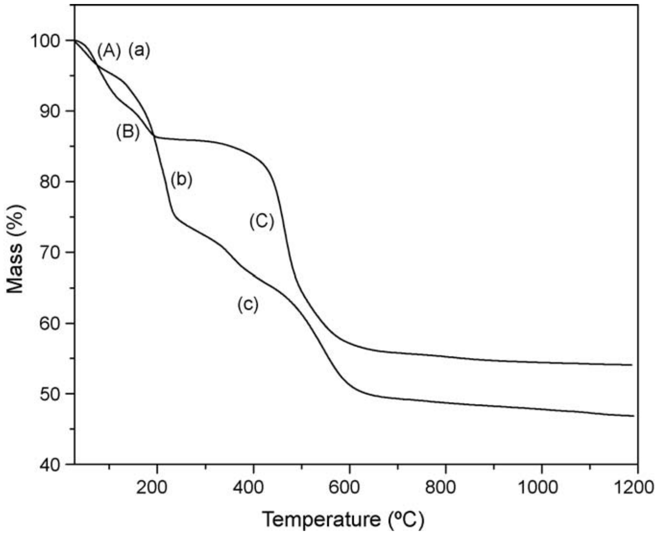

Fig. 8. TG curves for AC (—); ASCA(- - -) under atmosphere of nitrogen.

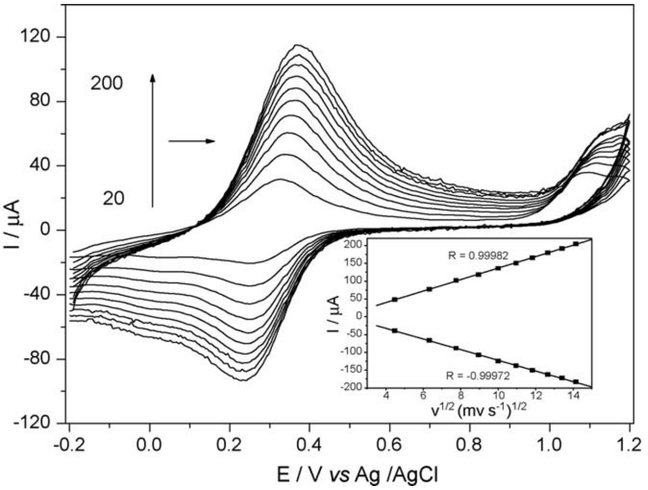

Fig. 9. Cyclic voltammograms of GPE–ASCA at different sweep rates (20–200 mV s^{-1}; NaCl 1.0 M). Inserted show the plot of I_p *vs.* ν.

The first weight loss was more pronounced for ASCA (9.10%) than for AC (4.34%) and was ascribed to the residual water. However, the second weight loss for ASCA (4.76%) was less pronounced than for AC (21.14%), starting at 107 °C and ascribed to the residual organic compounds included in the decomposition of these products. The third decomposition, which starts at 238 °C for ASCA and 201 °C for AC with weight loss of 30.2% and 24.8% was ascribed to the final decomposition, providing SiO_2 as residue.

The primary decomposition temperature (T_{dec}) and the char residue obtained from the TG curve can reflect the thermal stability of the material. The decomposition temperature (T_{dec}) is the temperature at which the weight loss is of about 5%. The 5% mass loss temperatures for ASCA was 123 °C. However, the primary decomposition temperature (half mass loss point) is about 637 °C. The char residue (N_2) of AC and ASCA is about 54.1% and 46.9%, respectively, as expected due to the high silica content.

Another characterization of ASCA was carried out by cyclic voltammetry, this result is illustrated in Fig. 9. The cyclic voltammogram of GPE–ASCA shows one redox couple and one irreversible process. The mid point potential ($E^{ox}_{1/2}$) (where $E^{ox}_{1/2} = E_{pa} + E_{pc}/2$ and E_{pa} = anodic peak potential and E_{pc} = cathodic peak potential) was around 0.30 V and an irreversible process occurred at 1.1 V (*vs.* Ag/AgCl; NaCl 1.0 M; $\nu = 20\,\mathrm{mV\,s^{-1}}$). An excellent linear relationship was verified between the first oxidation and reduction peak currents and square root scan rate from 20 to 200 mV s^{-1} (see graphic inset in Fig. 9), which is consistent and expected for the diffusion controlled electrode process. The ratio of the currents, I_{rev}/I_{fwd}, can be conveniently measured by the empirical method of Nicholson and Shain [40], which requires the evaluation of I_{pa}, I_{pc} and I_λ, where I_λ is the value of the current at the switching potential E_λ (where the direction of the CV scan is reversed). These quantities are then used to obtain the current ratio, I_{rev}/I_{fwd} in Eq. (1).

Table 2
Thermogravimetric steps for AC.

Steps	Temperature (°C)	%
A	30 at 115	4.34
B	115 at 201	21.4
C	201 at 650	24.8

Table 3
Thermogravimetric steps for ASCA.

Steps	Temperature (°C)	%
a	30 at 107	9.10
b	107 at 238	4.76
c	238 at 650	30.2

$$\left|\frac{I_{rev}}{I_{fwd}}\right| = \frac{I_{pc}}{I_{pa}} + \frac{0.485 \times (I_\lambda)}{I_{pa}} + 0.086 \qquad (1)$$

The I_{rev}/I_{fwd} and ΔE_p values were characteristic of a quasi-reversible redox process. Table 4 lists the main electrochemical parameters for these studies. The first and second process was described [41] by Eqs. (2) and (3), respectively. The electro inactivity nature of silicate cage was considered for this attribution [12]

$$\square\,Cu^{(I)}(N_3)_2 \rightarrow \square\,Cu^{(II)}(N_3)_2 + e^-\ \ (0.30\ \mathrm{V}) \qquad (2)$$

where

$$\square = [H_2N(CH_2)_3]_8Si_8O_{12}.$$

The main characteristic of the ASCA is a high sensitivity to the different biological compounds, for instance, nitrite, cysteine, ascorbic acid. Fig. 10 illustrates the sensitivity of ASCA to nitrite compound as an example of this material's application.

Fig. 10 displays cyclic voltammograms of GPE–ASCA in the absence (curve A) and presence (curve C) of nitrite. The carbon paste electrode (GPE) does not display any redox peaks in the potential range from −0.2 to 1.2 V. After the addition of nitrite, a substantial enhancement of the anodic peak current is observed at 1.0 V (curves C and B for Fig. 10). This behavior is more pronounced with GPE–ASCA than with GPE. In the GPE–ASCA, the peak current increased proportionately to the analyte concentration. This increase in the anodic current indicates an interesting sensitivity of nitrite compound by ASCA. The Cu(II) produced during the anodic scan chemically oxidizes these compounds while it is reduced to the Cu(I), which will again be oxidized to the Cu(II) electrochemically.

Table 4
Electrochemical parameters at several scan rate[a].

Vel ($mV\,s^{-1}$)	E_a (mV)	E_c (mV)	I_{pa} (μA)	I_{pc} (μA)	$E^{ox}_{1/2}$ (mV)	$(I_{pc})_0$ (μA)	I_λ (μA)	ΔE_p (mV)	I_{rev}/I_{fwd}	$(\nu)^{1/2}$ ($mV\,s^{-1}$)
20	330	259	47.8	−38.6	294	63.0	−26.8	71	1.20	4.47
40	340	257	77.2	−66.4	298	93.9	−39.8	83	1.03	6.32
60	348	255	102	−88.1	301	121	−47.1	93	1.02	7.75
80	352	253	118	−107	302	142	−53.1	99	0.99	8.94
100	363	251	136	−124	307	161	−59.5	112	0.98	10.0
120	365	243	150	−137	304	175	−64.1	122	0.96	10.9
140	367	239	166	−150	303	190	−69.8	128	0.96	11.8
160	369	237	180	−162	303	205	−82.7	132	0.93	12.6
180	373	235	192	−172	304	217	−90.1	138	0.92	13.4
200	376	233	204	−183	304	229	−98.1	143	0.90	14.1

[a] NaCl; 1.0 M.

The electrochemical oxidation of nitrite can be written as proposed by Guidelli and Casella [42,43]:

$$NO_2^- + H_2O \rightarrow NO_3^- + 2H^+ + 2e^- \quad (4)$$

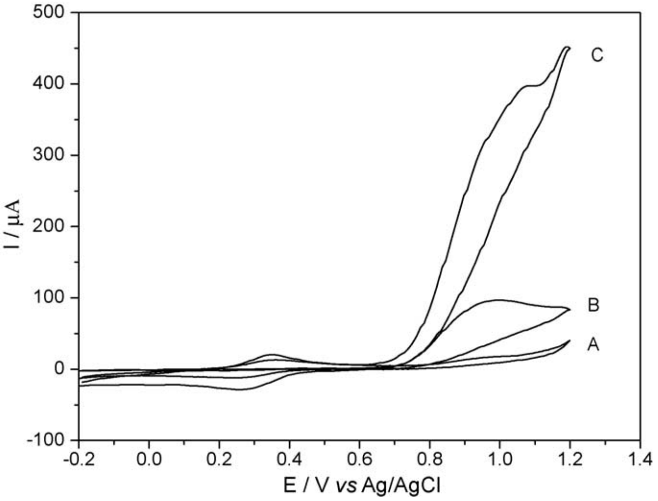

Fig. 10. Cyclic voltammograms of (A) GPE–ASCA without cysteine; (B) graphite paste electrode (GPE) after nitrite addition (2.5×10^{-3} mol L^{-1}); (C) GPE–ASCA after nitrite addition (2.5×10^{-3} mol L^{-1}) (NaCl 1.0 mol L^{-1}; $\nu = 20\,mV\,s^{-1}$).

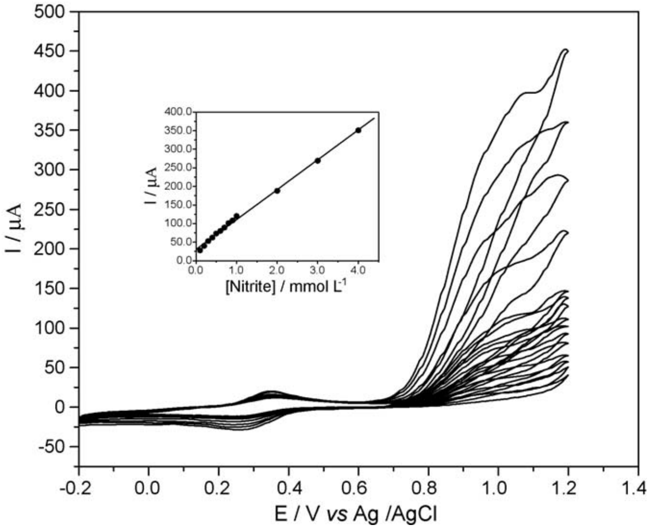

Fig. 11. Cyclic voltammograms of GPE–ASCA in the presence of nitrite (0.4–4.0 mol L^{-1}). Inserted: catalytic peak currents vs. nitrite concentration.

And the proposed catalytic process in the interface electrolyte solution at 1.1 V can be described as:

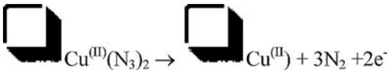

$$\text{Cu}^{(II)}(N_3)_2 \rightarrow \text{Cu}^{(II)} + 3N_2 + 2e^- \quad (5)$$

In addition, a calibration graph for the amount of nitrite *vs.* anodic current is shown in Fig. 11 (see the graphic inserted).

The modified electrode gives a linear range from 1.0×10^{-4} to 5.0×10^{-3} mol L^{-1} ($r = 0.998$) with detection limit of 2.1×10^{-4} mol L^{-1} and standard deviation of 5.6% for $n = 3$. For the determination of nitrite the amperometric sensitivity was 8.04 mA/mol L^{-1}.

The linear dependence of the calibration curve in Fig. 11 (graphic inserted) suggests that the response of the modified electrode with ASCA is appropriate for quantitative nitrite determination even in the millimolar concentration range. Similarly, when compared to the methods involving mercury electrodes, the calibration plot crosses the abscissa, presumably due to the interference of trace heavy metal in the supporting electrolytes [44], but this does not interfere with the success for determining nitrite compounds by addition methods. The presence of organic compounds, such as 500-fold hydrazine and 50-fold dopamine, does not interfere with the determination of 0.25 mM nitrite. The ASCA modified electrode was stable and reproducible. A 10.5% decrease of the current response was found for 6 weeks.

5. Conclusion

ASCA was synthesized from copper octa(3-aminopropyl)octasilsesquioxane following its subsequent reaction with azide ligands. The precursor and novel compound were characterized by FTIR, NMR, XRD, EPR, SEM, TG analyses and voltammetric techniques. AAS, FTIR, NMR, XRD and EPR spectroscopies indicate that ligands successfully complex to the metal center in the silsesquioxane cage. The presence of complex Cu/N_3^- in octameric cube, confers a loss of crystallinity and relative thermal stability to the material. The cyclic voltammogram of the modified graphite paste electrode with ASCA (GPE–ASCA), showed one redox couple with formal potential ($E^{ox}_{1/2}$) = 0.30 V and an irreversible process at 1.1 V (*vs.* Ag/AgCl; NaCl 1.0 M; $\nu = 20\,mV\,s^{-1}$). The novel nanostructured material is very sensitive to nitrite concentrations. The composite could be employed as an electrochemical sensor for biological compounds such as nitrite, and should therefore deserve more attention.

Acknowledgements

The authors would like to express their gratitude for the financial support by the Fundação de Amparo à Pesquisa do Estado de São Paulo (FAPESP-Proc. 03/12882-6; 01/04494-0 and 92/3515-3).

References

[1] International Union of Pure and Applied Chemistry (IUPAC), 67 (1995) 1336.

[2] R.H. Baney, M. Itoh, A. Sakakibara, T. Suzuki, Chem. Rev. 95 (1995) 1409.

[3] P.D. Lickiss, F. Rataboul, Adv. Organomet. Chem. 57 (2008) 1.

[4] M.G. Voronkov, V.L. Lavrent'yev, Top. Curr. Chem. 102 (1982) 199.

[5] L. Guizhi, L. Wang, H. Ni, C.U. Pittman Jr., J. Inorg. Organ. Polym. 11 (2001) 123.

[6] H.V. Tran, R.J. Hung, D.A. Loy, D.R. Wheeler, J. Byer, W. Conley, C.G. Willson, Abstr. Pap. Am. Chem. Soc. 221 (2001) 283.

[7] C. Zhang, R.M. Laine, J. Am. Chem. Soc. 122 (2000) 6979.

[8] X. Gong, C. Soci, C.Y. Yang, A.J. Heeger, S. Xiao, J. Phys. D: Appl. Phys. 39 (2006) 2048.

[9] F. Carniato, E. Boccaleri, L. Marchese, A. Fina, D. Tabuani, G. Camino, Eur. J. Inorg. Chem. 4 (2007) 585.

[10] S. Iyer, D.A. Schirald, Macromolecules 40 (2007) 4942.

[11] F. Carniato, A. Fina, D. Tabuani, E. Boccaleri, Nanotechnology 19 (2008) 475701.

[12] D.R. do Carmo, N.L. Dias-Filho, N.R. Stradiotto, Appl. Surf. Sci. 235 (2004) 348.

[13] K.J. Haxton, D.J. Cole-Hamilton, R.E. Morris, J. Chem. Soc., Dalton Trans. (2004) 1665.

[14] Q. Pan, L. Gao, X. Chen, X. Fan, Q. Zhou, Macromolecules 40 (2007) 4887.

[15] L. Ropartz, R.E. Morris, D.F. Foster, D.J. Cole-Hamilton, J. Mol. Catal. A: Chem. 182 (2002) 99.

[16] K. Pielichowski, B. Janowski, J. Pielichowski, Supramol. Pol. 201 (2006) 225.

[17] D.R. do Carmo, L.L. Paim, N.L. Dias Filho, N.R. Stradiotto, Appl. Surf. Sci. 253 (2007) 3685.

[18] D.M.L. Goodgame, S. Kealey, P.D. Lickiss, A.J.P. White, J. Mol. Struct. 890 (2008) 232.

[19] W.Z. Chen, Y.T. Tsai, T.H. Lin, Appl. Phys. Lett. 94 (2009) 201114.

[20] Q.W. Pan, X.H. Fan, X.F. Chen, Q.F. Zhou, Prog. Chem. 18 (2006) 616.

[21] M. Moran, C.M. Casado, I. Cuadrado, Organometallics 12 (1993) 4327.

[22] L. Losada, M.P. Garcıa Armada, B. Alonso, B. Gonzalez, C.M. Casado, J. Zhang, J. Organomet. Chem. 689 (2004) 2789.

[23] H. Schimidt, Mater. Res. Soc. Symp. 171 (1990) 3.

[24] S. Kritgen, L. Mojet, H.C.L. Abbenhuis, J.H.C. Van Hoof, R.A. Van Santen, Phys. Chem. Chem. Phys. 1 (1999) 361.

[25] D.R. do Carmo, N.L. Dias Filho, N.R. Stradiotto, Mater. Res. Bull. 42 (2007) 1811.

[26] R.Y. Kannan, H.J. Salacinski, P.E. Butler, A.M. Seifalian, Acc. Chem. Res. 3 (2005) 879.

[27] H.C.L. Abbenhuis, Chem. Eur. J. 6 (2000) 25.

[28] U. Simon, G. Schon, G. Schmid, Angew. Chem. Int. Ed. Engl. 32 (1993) 250.

[29] O. Kahn, Molecular Magnetism, VCH, Weinheim, 1993.

[30] J. Ribas, A. Escuer, M. Monfort, R. Vicente, R. Cortés, L. Lezama, T. Rojo, Coord. Chem. Rev. 193 (1999) 1027.

[31] P.S. Mukherjee, T. Maji, A. Escuer, R. Vicente, J. Ribas, G. Rosair, F.A. Mautner, N.R. Chaudhuri, Eur. J. Inorg. Chem. (2002) 943.

[32] A.K. Sra, J.-P. Sutter, P. Guionneau, D. Chasseau, J.V. Yakhmi, O. Kahn, Inorg. Chim. Acta 300 (2000) 778.

[33] T.K. Karmakar, S.K. Chandra, J. Ribas, G. Mostafa, T.H. Lu, B.K. Ghosh, Chem. Commun. (2002) 2364.

[34] R.M. Laine, M.C. Gravel, Polym Prepr. 38 (1997) 155.

[35] X.-J. Lin, Z. Shen, Y. Song, H.-J. Xu, Y.-Z. Li, X.-Z. You, Inorg. Chim. Acta 358 (2005) 1963.

[36] R.A. Mantz, P.F. Jones, K.P. Chaffee, J.D. Lichtenhan, J.W. Gilman, I.M.K. Ismail, M.J. Burmeister, Chem. Mater. 8 (1996) 1250.

[37] F. Kattou, G. Aptel, D.J. Jones, B. Deroid, J. Rosière, J.-V. Zancheta, Micropor. Mesopor. Mater. 47 (2001) 231.

[38] G. Facchin, E. Kremer, E.J. Baran, E.E. Castellano, O.E. Piro, J. Ellena, A.J. Costa-Filho, M.H. Torre, Polyhedron 25 (2006) 2597.

[39] A. Bencini, D. Gatteschi, EPR of Exchange Coupled Systems, Springer-Verlag, Berlin, 1990.

[40] R.S. Nicholson, I. Shain, Anal. Chem. 36 (1964) 706.

[41] J. Xu, G.M. Swain, Anal. Chem. 70 (1998) 1502.

[42] R. Guidelli, F. Perdegola, G. Rospi, Anal. Chem. 44 (1972) 745.

[43] I.G. Casella, A.M. Salvi, Electroanalysis 9 (1997) 596.

[44] T.M. Florence, J. Electroanal. Chem. 97 (1979) 237.